

duneuro - A software toolbox for forward modeling in neuroscience

Andreas Nüßing^{1,2,3}, Maria Carla Piastra^{2,4}, Sophie Schrader², Tuuli Miinalainen^{5,6}, Sampsa Pursiainen^{5,7}, Heinrich Brinck³, Carsten H. Wolters², Christian Engwer^{1*}

1 Applied Mathematics: Institute for Analysis and Numerics, University of Münster, Germany

2 Institute for Biomagnetism and Biosignalanalysis, University of Münster, Germany

3 Westfälische Hochschule, University of Applied Sciences Recklinghausen, Germany

4 Radboud University Nijmegen Medical Centre, Donders Institute for Brain, Cognition and Behaviour, The Netherlands

5 Laboratory of Mathematics, Tampere University of Technology, Finland

6 Department of Applied Physics, University of Eastern Finland, Kuopio, Finland.

7 Laboratory of Signal Processing, Tampere University of Technology, Finland

* christian.engwer@uni-muenster.de

Abstract

This paper describes *duneuro*, a software toolbox for forward modeling in neuroscience. Its purpose is to provide extendible and easy-to-use interfaces and enable a closer integration into existing analysis pipelines. It provides implementations of fitted and unfitted finite element methods and makes use of the Dune framework. The forward problems consist of the electroencephalography (EEG) and magnetoencephalography (MEG) forward problems. For the incorporation into existing analysis pipelines, Python and Matlab interfaces are provided. The practical use is demonstrated on a source analysis example of evoked potentials.

1 Introduction

We present *duneuro*, a software toolbox for forward modeling in neuroscience. Its main focus is to provide an extendible and easy-to-use framework for using various finite element methods for different neuroscientific applications, such as the EEG or MEG forward problem [1, 2].

The general view on a software toolbox can be split into two parts: the user perspective and the developer perspective. From the perspective of a user, the toolbox should

be accessible and easy to use. Similar methods should work in a similar way through a common interface. When considering the solution of the EEG forward problem, it should be possible to quickly exchange the discretization scheme. The user should not be confronted with the high complexity of a C++ finite element code. Additionally, it should be possible to embed the forward approach into an already existing processing pipeline. From the point of view of a developer, who wants to implement different discretization schemes or extend already existing approaches, further aspects are important. As different finite element methods share several subcomponents, such as the representation of the computational domain or the solver of the linear system, the toolbox should bundle the different implementations and enable code reuse. The toolbox should be extendible, especially with respect to common variable components. In addition, as there are already several libraries offering codes for finite element computations, it would be advantageous to make use of existing components and benefit from existing maintenance and testing infrastructure.

In order to perform analysis of EEG or MEG data, different open source software packages offer tools to implement a complete processing pipeline such as the Matlab-based toolboxes FieldTrip [3], Brainstorm [4] and Zeffiro [5], the Python-based toolbox MNE-Python [6] or the C++ code MNE [7]. The toolbox SimBio¹ offers a broad range for forward and inverse methods for EEG and MEG analysis. Recently, a small subset of its functionality has been integrated into FieldTrip [8]. With respect to the finite element method, only first order Lagrangian elements are implemented in SimBio. Due to its structure, extending the code to support different discretization schemes would be error-prone and time-consuming. In addition, there are well-tested and established general purpose software toolboxes for finite element computations.

One existing library for finite element computations is the *distributed and unified numerics environment (Dune)*². More precisely, it is a general purpose open-source C++ library for solving partial differential equations using mesh-based methods. It is extendible by offering a modular structure and providing abstract interfaces and separation between data structures and algorithms. Due to the modular structure, a user of Dune only has to use those modules that are needed. At the core of the Dune library is an abstract definition of a grid interface [9, 10]. Using the abstract interface allows writing reusable code that is independent of the concrete implementation of the grid or the type of the grids elements. Then the identical code can be used in multiple spatial dimensions and for tetrahedral, hexahedral or other element types.

The duneuro library presented in this paper makes use of several existing Dune modules. For representing geometry-conforming tetrahedral and hexahedral meshes, we use the grid implementations provided by the dune-uggrid module [11]. In order to reduce the memory consumption and to simplify the user-code when using a geometry-adapted hexahedral mesh [12], we use the dune-subgrid module to extract parts of a mesh that

¹<https://www.mrt.uni-jena.de/simbio>

²<http://www.dune-project.org>

is given as a segmented voxel image [13]. The discretization of the partial differential equation makes use of the dune-pdelab module [14]. In dune-pdelab, many different discretization schemes along with appropriate finite elements are implemented allowing a rapid prototyping of new models. It offers abstractions for the concept of a function space on a grid or for the linear operator used in the discretization. The implementation of the unfitted discontinuous Galerkin method is provided in the dune-udg module [15]. This module has been extended to support also the CutFEM method presented in [16]. One component of the unfitted finite element methods is the integration over implicitly defined domains, which is performed using the C++ library tpmc³. For the solution of the linear system, we make use of the *iterative solver template library (ISTL)* offered by the dune-istl module [17].

In the following, we first give a short summary on the background of solving the EEG and MEG forward problems with finite element methods in Section 2. This is followed by a general description of the toolbox and its use of existing frameworks for solving partial differential equations. In Section 3 we introduce the main concepts of different interfaces used within the library. Section 4 describes a method for localizing elements within a tessellation based on a global coordinate. The interaction of a user with duneuro is done through bindings with a scripting language, which will be presented in Section 5. In Section 6, we use the duneuro toolbox to calculate forward solutions which are subsequently used for source analysis on EEG data obtained from a somatosensory experiment. Finally, a short conclusion is given in Section 7.

2 Background

In this section we present the background for solving the EEG and MEG forward problems with finite element methods.

The EEG forward problem The aim of the EEG forward problem is to compute the electric potential u in a domain $\Omega \subset \mathbb{R}^d$. It can be formulated using Poisson's equation:

$$\nabla \cdot \sigma \nabla u = \nabla \cdot j^p \quad \text{in } \Omega \quad (1)$$

$$\langle \sigma \nabla u, n \rangle = 0 \quad \text{on } \partial\Omega, \quad (2)$$

where $\sigma : \Omega \mapsto \mathbb{R}^{3 \times 3}$ denotes the symmetric and positive definite conductivity tensor, j^p denotes the primary current density and n denotes the unit outer normal on $\partial\Omega$. The current source is usually modeled as a current dipole at a position $x_{dp} \in \Omega$ with the dipole moment $M \in \mathbb{R}^d$. With the use of the delta distribution $\delta_{x_{dp}}$ centered at x_{dp} , the current dipole leads to the source term

$$\nabla \cdot j^p = M \cdot \nabla \delta_{x_{dp}}.$$

³<http://github.com/tpmc>

Finite element methods for the EEG forward problem Several finite element methods have been proposed to solve the EEG forward problem. A common basis for these methods is the tessellation of the computational domain Ω . The domain is partitioned into a set of elements of simple shape, such as tetrahedrons or hexahedrons. Depending on the concrete method, certain regularity assumptions are imposed on the tessellation, such as not containing hanging nodes. For details on the precise definition of a tessellation we refer to [18]. In the following, we will denote a tessellation of Ω by $\mathcal{T}_h(\Omega)$. Here, $h \in \mathbb{R}$ denotes the maximal diameter of a mesh element.

One main difference between several finite element methods is the discrete representation of the potential u and the formulation of the discrete representation of Poisson's equation. We will not present the mathematical rigorous definition of the different methods but refer to the respective publications that introduced the methods for solving the EEG forward problem. The conforming finite element method using Lagrangian elements represents the potential as a continuous, piecewise polynomial function [19, 20, 21, 22, 23, 24, 25, 26, 27, 28, 29, 30]. For the discretization of the equation, the classical weak formulation is used directly. In contrast, the discontinuous Galerkin method does not enforce the continuity of the potential in its function definition but instead, incorporates the continuity weakly through the use of a modified weak formulation [31]. Using this approach, it gains continuity of fluxes on the discrete level. The mixed finite element method transforms the second order Poisson's equation into a system of first order equation, introducing an additional unknown for the electric field [32].

The finite element methods described above have in common that they use a tessellation which resolves the computational domain Ω . Recently, two finite element methods have been introduced for solving the EEG forward problem that instead use a tessellation of an auxiliary domain $\hat{\Omega}$ which is independent of Ω . The conformity of the solution to the domain Ω is incorporated weakly by modifying the discrete weak formulation. The CutFEM method uses a function representation that is continuous on each isotropically homogenized tissue compartment [33, 16]. The unfitted discontinuous Galerkin method additionally transfers the continuity constraint within each subdomain to the weak formulation [34, 35, 36].

Due to the difference in representing the discrete function and the different properties of these representations, different strategies for discretizing the dipolar source term have to be taken into account. Usually, the derivative of the delta distribution cannot be directly applicable to a discrete test-function. Several different approaches for the various finite element methods have been proposed in the literature. For the conforming finite element methods, the partial integration approach [24, 37], the St. Venant approach [12, 21, 38], the full and projected subtraction approach [39, 25, 26] and the Whitney approach [40, 22, 41, 42] have been introduced. Similar approaches have been presented for the discontinuous Galerkin method, however their exact formulation differs, due to the different discretization approach. These approaches are the partial integration approach [43], the Venant approach [16] and the full and localized subtraction approach [31, 16]. For the unfitted finite element methods both the partial integration approach

and approaches following the principle of St. Venant have been adopted [16].

The discretization of the EEG forward problem leads to a system $Ax = b$ to be solved for $x \in \mathbb{R}^n$. In order to speed up the computation of the solution to the EEG forward problem, we first note that in order to compute a lead field matrix, it is not necessary to know the potential in the interior of the domain Ω , but only the evaluation at the sensor positions on the boundary. For a given source, this leads to a potential vector $U \in \mathbb{R}^N$, where $N \in \mathbb{N}$ denotes the number of sensors. Given a solution $x \in \mathbb{R}^n$, the evaluation can be represented by a linear map $R \in \mathbb{R}^{N \times n}$ as $U = Rx$. Inserting $x = A^{-1}b$ and defining $T := RA^{-1}$ results in $Tb = U$. This means, once T is known, the EEG forward problem can be solved by computing the right-hand side vector b and performing a matrix-vector multiplication. The matrix $T \in \mathbb{R}^{N \times n}$ is called the (EEG) *transfer matrix*. By exploiting the symmetry of the discrete operator A , the transfer matrix can be computed row-wise by solving $AT^t = R^t$ using the N rows of R as the right-hand sides. Thus, for the computation of the transfer matrix, the linear system has to be solved once for every sensor location.

MEG In addition to the EEG forward problem, the toolbox provides methods to solve the MEG forward problem [44]. Given the electric potential u , the secondary magnetic field B at a position $y \in \mathbb{R}^d$, resulting from the volume current $\sigma \nabla u$, can be expressed using the law of Biot-Savart [45]:

$$B(y) = \frac{\mu_0}{4\pi} \int_{\Omega} \sigma \nabla u \times \frac{y - x}{\|y - x\|^3} dx,$$

where \times denotes the three-dimensional cross product.

For the conforming Galerkin method (CG-FEM) this integral can be directly evaluated using the discrete representation of the potential u_h . Results for the MEG approach for the discontinuous Galerkin method (DG-FEM) in [44] indicate, that a direct usage of $\sigma \nabla u_h$ leads to suboptimal accuracies. Instead, the numerical flux of the discontinuous Galerkin method should be used, which is defined as

$$\{\sigma \nabla u_h\} - \frac{\eta}{h} \llbracket u_h \rrbracket$$

(for details, see [44]). In order to provide a single implementation for the integration using both flux representations, we split the MEG forward solution into two parts: the projection of the flux into a vector valued function space W_h and the evaluation of the integral functional for functions in W_h . In [44], a lowest order Raviart-Thomas space was used for representing the continuous numerical flux, while a space representing gradients of piecewise multi-linear functions has been employed to represent the physical flux. The discrete potential u_h is given as

$$u_h(x) = \sum \alpha_i \phi_i(x)$$

and the discrete representation of the flux is given as

$$\sigma \nabla u_h(x) \approx \sum \beta_j \psi_j(x).$$

Using this discrete representation of the flux, the MEG integral for a fixed sensor position $y \in \mathbb{R}^d$ can be evaluated by computing

$$\text{MEG}(u, y) = \sum \beta_j \frac{\mu_0}{4\pi} \int_{\Omega} \psi_j \times \frac{y - x}{\|y - x\|^3} dx =: \langle S(y), \beta \rangle.$$

The computation of the coefficients for the flux based on the coefficients of the discrete potential can be expressed as a linear operator

$$\beta = P\alpha.$$

The exact definition of this linear operator depends on the interpolation scheme in the vector valued function space. Combining the projection and the integral evaluation, the MEG solution can be obtained from a discrete EEG solution by computing

$$\text{MEG}(u, y) = \langle P^t S(y), \alpha \rangle.$$

Using this representation, a transfer matrix approach for MEG can be defined following the description above, where $P^t S(y)$ takes the role of the restriction operator, mapping the discrete solution to the sensor values. The MEG forward solution is available for any source model. However, note that when using a subtraction approach, the resulting MEG solution does not include the contributions of the singularity potential.

3 Library Interfaces

In this section we present in detail several subcomponents and interfaces of the duneuro toolbox and give information on the extendibility of each component. We describe the driver interface, the discretization of the forward model and the EEG source model and provide information about the MEG implementation.

The EEG-MEG Driver Interface As described above, there are several different discretization schemes available for solving the EEG forward problem and each scheme provides different source models. The finite element methods presented here can be split into two different categories: the *fitted* and *unfitted* discretization methods. The fitted category refers to a discretization method that uses a grid whose geometry is fitted to the model geometry. The basis of this approach is a `VolumeConductor` class that stores the grid along with the conductivity tensor of each grid element. Currently, there are two different fitted discretization schemes implemented in duneuro: the conforming Galerkin (CG-FEM) and the discontinuous Galerkin (DG-FEM) finite element methods. Methods

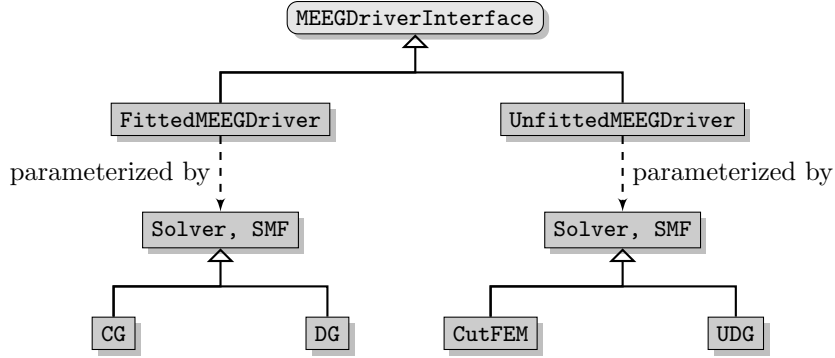


Figure 1: Diagram showing the structure of the driver interface and its implementations. The `SourceModelFactory` is abbreviated as `SMF`.

that fall into this category but are not yet available are mixed finite element methods or finite volume schemes. The unfitted category refers to a discretization method that uses a grid which is independent of the model geometry and employs the model geometry weakly. The model geometry is provided implicitly via level-set functions and considered in the weak formulation. The currently implemented discretization schemes in the unfitted category are: the CutFEM method and the unfitted discontinuous Galerkin method. From the user perspective of a software framework, it should be simple and intuitive to change from a fitted to an unfitted discretization or between different discretization schemes within each category. For example switching from CG-FEM to DG-FEM should not require fundamental changes in the user code. A further consideration when designing the interface of the software is the way the user will interact with it. As described in more detail below, we want to provide bindings to languages a potential user is already familiar with, such as Python or Matlab. In order to simplify both, the overall user interface as well as the process of creating such bindings, we define a single coarse grained interface class to interact with the internal toolbox. This interface class is called the `MEEGDriverInterface`. It describes the general concepts of solving EEG and MEG forward problems. Each of the two discretization categories is implemented by its own driver class, the `FittedMEEGDriver` and the `UnfittedMEEGDriver` respectively. Figure 1 shows a general diagram of the `MEEGDriverInterface`. For each category, the implementation of the discretization scheme is provided via two template parameters: a `Solver` and a `SourceModelFactory`. The purpose of the solver class is to bundle the handling of the system matrix and the solution of the resulting linear system. The source model factory will construct source models whose purpose is the assembly of the right-hand side. Both, the solver and the source model factory, are further described below. The user of the toolbox will not directly interact with the implementation of the drivers, but only with the driver interface class.

The Solver and the Source-Model-Factory The purpose of the solver class is the assembly of the system matrix and the solution of the linear system. It contains the discretization scheme as well as the necessary function spaces for representing discrete functions. The main interface method is a `solve` method which, given a right-hand side vector, solves Poisson’s equation and returns the discrete solution. Several forward problems in bioelectromagnetism, e.g., the EEG forward problem, electric or magnetic stimulation or the computation of a transfer matrix, mainly differ with respect to the right-hand side of the linear system. The solver class can thus be reused for any such purpose. By using a single solver class, the system matrix has to be assembled only once and can be reused for further purposes. As the different discretization schemes differ in the way the matrix is stored, e.g., with respect to the blocking scheme of the matrix entries, this information is hidden from the interface. The purpose of the source model factory is to construct the different source models dynamically based on a configuration provided by the user. All source models provide a common interface which is described below.

We will illustrate the extendibility with respect to the discretization scheme using the example of a mixed finite element method. `MixedFEM` is based on a first order representation of Poisson’s equation and employs unknowns for both, the potential and the electric field. It derives a weak formulation and uses scalar and vector-valued finite elements on a geometry conforming grid as a discretization. It thus falls into the category of fitted discretization schemes. In order to use the described `FittedMEEGDriver`, one needs to provide two components: a `MixedFEMSolver` and a `MixedFEMSourceModelFactory`. The `MixedFEMSolver` contains the discretization of the stiffness matrix as well as the definition to solve the resulting linear system. The implementation of such a solver class is heavily based on the `dune-pdelab` module, which contains for example the implementations of the local basis functions. The `MixedFEMSourceModelFactory` offers a method to create different source models for the `MixedFEM` approach, whose purpose is then to assemble the right-hand side vector for a given source position. In [32], two different source models have been presented: a *direct approach* and a *projected approach*. Finally, one has to provide means to evaluate a discrete solution at electrode positions along with the resulting right-hand side of the transfer matrix approach. Once these components are implemented, the features of the driver, e.g., computing a transfer matrix or solving the EEG forward problem, are available.

Source Models For each discretization method, there are several different source models that are used to discretize the mathematical point dipole. The common task of these source models can be stated as: given a dipole position and a dipole moment, assemble the right-hand side vector. This right-hand side vector will then be passed on to the respective solver class described above. As there is still research ongoing and new source models are being developed, it should be easy to provide an additional source model without having to modify the existing code. In addition, it should be possible to choose

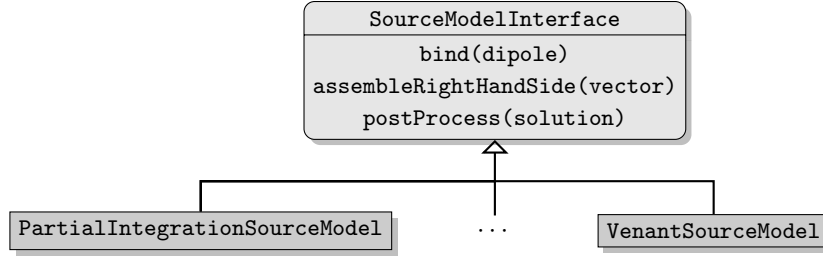


Figure 2: The structure of the source model interface and its implementations.

the source model at runtime, both for investigating the effects of different source models as well as ruling out the source model as a source of errors. Some source models, such as the subtraction approach, do not provide a right-hand side for the full potential, but need to apply an additional post-processing step to the resulting solution in order to obtain the full potential. For the subtraction approaches, this post-processing step consists of adding the singularity potential to the correction potential. As this post processing step depends on the type of the source model and the user should have the option to turn off the post-processing, it is provided as a method of the source model interface. Figure 2 shows a diagram of the general `SourceModelInterface` along with its implementations.

A main advantage of the direct source models such as the partial integration approach or the Venant approaches, is the sparsity of the right-hand side. When stored inside a sparse vector container, the time for applying the transfer matrix, i.e., multiplying the right-hand side with the transfer matrix, can be reduced. The complexity is $\mathcal{O}(M)$, where M denotes the number of mesh elements. The constant is proportional to the number of non-zero entries of the right-hand side. The latter is usually independent of the mesh resolution. For indirect source models such as the subtraction approach, using the same data type as for the sparse source models would introduce an additional overhead. Thus, in order to be able to handle dense and sparse vector types for the right-hand side, the vector type is provided as a template parameter of the source model interface.

We will illustrate the extendibility with respect to the source models on the example of a modified subtraction approach for CG-FEM. In [16] a modification of the subtraction approach has been presented: the *localized subtraction approach*. It restricts the contribution of the singularity part of the potential to a patch around the source location. As the functions within a DG-FEM discretization can be discontinuous, they can directly capture the jump occurring at the boundary of the patch. For a CG-FEM discretization, such jumps can not be directly resolved and thus the localization scheme has to be modified. Instead of using a restriction of the singularity contribution to the patch, one can multiply the singularity contribution with a function that linearly interpolates within an interface zone of the patch between the singularity potential and zero. A source model implementing this localized subtraction approach would provide a class fulfilling

the source model interface. Within the `bind` method, the local patch would be created and the linear interpolation in the interface zone could be constructed. The implementation of the `assembleRightHandSide` method contains the integration of the different model terms, resulting in the right-hand side. The `postProcess` method adds the singularity potential to the correction potential on the local patch.

4 Element Localization

A common subtask when assembling the right-hand side for a given dipole is the localization of the mesh element containing the dipole. For a sparse source model, this is especially relevant, as the time of assembling the right-hand side is usually constant, once the dipole element has been found. The complexity of the right-hand side assembly thus strongly depends on the complexity of the method that is used for finding the dipole element. The most straight forward approach is given by a linear search among the mesh elements. Assuming an ordering of the mesh elements, we evaluate for each element of the mesh if it contains the dipole position. Once the result of the evaluation is positive, we return this element. This algorithm has an average and worst case complexity of $\mathcal{O}(M)$, where M denotes the number of mesh elements.

A first step to speed up the localization can be found by using geometric information when iterating the mesh elements instead of using a fixed ordering [46]. The method presented here is called *edge hopping*:

1. Start at a given mesh element and iterate over all faces of the current element.
2. Compute the relative position of the dipole location and the hyperplane induced by the face center and its outer normal.
3. If the dipole lies in normal direction, continue the search at step 1 with the neighboring element if such an element exists.
4. If the face has no neighboring element, the dipole lies outside of the mesh or the mesh is not convex. Terminate the search.
5. If the dipole lies in the opposite direction, continue at step 2 with the evaluation of the next face.
6. If the dipole lies on the inside of all faces of the current element, the dipole element has been found.

A requirement of the edge-hopping method is the convexity of the mesh, that is usually only fulfilled by the multi-layer sphere models, and not by the realistically shaped head models. However, as the algorithm monotonously moves closer to the dipole element, we only need convexity of the mesh in a sphere around the dipole location and the starting point of the iteration. As the considered sources lie in the gray matter compartment,

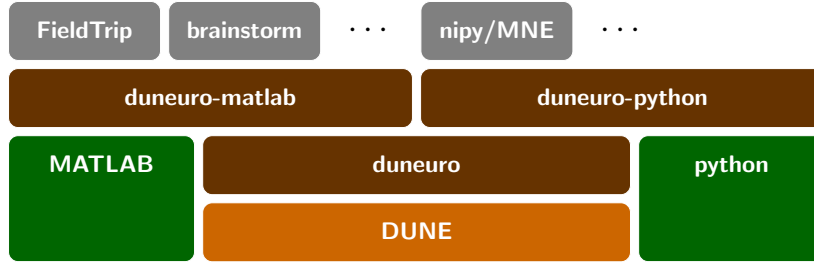


Figure 3: Relation of the duneuro modules with respect to Dune, external software and downstream libraries.

that is completely enclosed by the skin, we can easily find such a sphere around the source locations if the starting location is close to the source position. In order to find an element that is close to the source location, we insert the element centers into a *k-d Tree*, that is a datastructure to efficiently perform nearest neighbor searches [47]. It does so by recursively splitting the set of element centers along the Cartesian directions. Even though the center of the element which is closest to the dipole location does not have to belong to the element containing the dipole, it can be assumed to be close to the desired element. It thus offers an efficient starting point for the edge-hopping algorithm.

5 Interface to Scripting Languages

In this section we describe the interaction of a user with the duneuro library.

A common approach is to provide a compiled binary executable that the user is able to call directly. This executable would then load the data provided by the user from the hard disk, perform the desired computation and write the computed result back to the hard disk. As different users might want to perform different sets of computations, the computations to be performed can be configured by the user, either through command line parameters or through a configuration file. An advantage of this approach is its very simple and straight forward usage, similar to any other executable on the operating system. There is no need for additional packages or additional software and the executable can be used directly by the user. However, the computation of the solution to the forward problems is usually only a small part in a longer pipeline for source analysis. This pipeline usually consists of the data measurements and pre-processing steps and the forward solution is part of an inverse estimation process. When using the library directly in an executable, one has to provide methods for reading any input data as well as writing out the resulting output. Similarly, the configuration has to be transferred to the executable by the user.

A more convenient way to use the provided library can be found by offering bindings to

```

import duneuro as dp
config = {
    'type' : 'fitted',
    'solver_type' : 'cg',
    'element_type' : 'tetrahedron',
    'volume_conductor' : {
        'grid.filename' : 'path/to/grid.msh',
        'tensors.filename' : 'path/to/tensors.dat'
    }
}
driver = dp.MEEGDriver3d(config)

```

Listing 1: Example Python script for creating an `MEEGDriver`.

a scripting language such as Matlab⁴ or Python⁵. For both languages there are already existing software frameworks for processing EEG and MEG data [6, 3, 4]. Thus, by providing direct bindings one can include the forward modeling approach directly into an existing analysis pipeline. An example for such an integration is presented in [8], where the authors introduce a pipeline for performing source analysis using the conforming finite element method together with the classical Venant source model. The forward models are implemented using the SimBio software⁶ and integrated into the Matlab-based FieldTrip-toolbox⁷. The Python and Matlab bindings for the `duneuro` module are provided in separate Dune modules: *duneuro-py* and *duneuro-matlab*, respectively. The purpose of both modules is to translate the input data given as data structures in the respective programming language and translate them into the C++ counterparts. For some cases, this translation can be performed without copying any data, which is especially relevant for large matrices such as the transfer matrix. An example of the driver construction in a Python script is shown in Listing 1. The configuration of the discretization is provided as a python dictionary and the mesh is loaded from a file. Alternatively, the mesh can also be provided directly by specifying the vertices, elements, labels and conductivity tensors. Note that the discretization method, in this case `cg`, is provided as a parameter in the configuration. By changing it to `dg` and adding the necessary additional parameters such as the penalty parameter η , one can directly use the discontinuous Galerkin method through the same interface. Thus, once a user is able to use the `duneuro` library for any discretization method, a switch to a different discretization method can be directly performed. Listing 2 shows the same construction of the driver object as in Listing 1 using the Matlab interface. The general structure of the Matlab script is similar to the

⁴<https://www.mathworks.com>

⁵<https://www.python.org>

⁶<https://www.mrt.uni-jena.de/simbio>

⁷<http://www.fieldtriptoolbox.org>

```

cfg = [];
cfg.type = 'fitted';
cfg.solver_type = 'cg';
cfg.element_type = 'tetrahedron';
cfg.volume_conductor.grid.filename = 'path/to/grid.msh';
cfg.volume_conductor.tensors.filename = 'path/to/tensors.dat';
driver = duneuro_meeg(cfg);

```

Listing 2: Example Matlab script for creating an `MEEGDriver`.

Python script. The main differences are the use of Matlab syntax and the replacement of the Python dictionary by a Matlab struct array. Even though the wrapper code for creating the driver object is different, both scripting languages interface the C++ library and use the same code base.

6 Example: Source Analysis of Somatosensory Evoked Potentials

As a practical example the forward solutions of `duneuro` are used to perform a dipole scan on somatosensory evoked potentials using the CutFEM method. A right-handed, 49 years old, male subject participated in an electric stimulation experiment of the right median nerve with simultaneous EEG recordings. The EEG was measured using 74 electrodes, whose positions were digitized using a Polhemus FASTTRAK device⁸. The subject was stimulated in supine position in order to reduce modeling errors due to brain movement, because the corresponding MRI for head volume conductor modeling was also measured in supine position [48]. In total, 1200 stimuli were applied, each with a duration of 200 ms. The inter-stimulus interval was randomized in the range of 350 ms to 450 ms. The EEG data was preprocessed using a band-pass filter from 20 Hz to 250 Hz and notch-filters at 50 Hz and harmonics to reduce power-line noise. After removing one bad channel the remaining trials were averaged to produce the evoked potential data. Figure 4 shows a butterfly plot of the resulting time series of the averaged potentials as well as a topography plot of the potential measured at the electrodes at the peak of the P20 component at the time point of 25.8 ms.

Using a 3 T MRI scanner (Siemens Medical Solutions, Erlangen, Germany), T1-weighted and T2-weighted MRI sequences were measured. Based on these MRI images, a six-compartment voxel segmentation has been constructed, distinguishing between skin, skull compacta, skull spongiosa, csf, gray matter and white matter using SPM12⁹ via

⁸<https://polhemus.com>

⁹<http://www.fil.ion.ucl.ac.uk/spm/software/spm12>

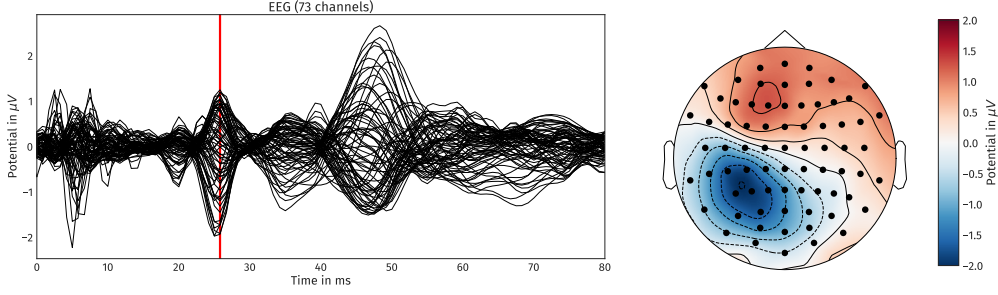


Figure 4: Left: Butterfly plot of the somatosensory evoked potentials. The vertical red line indicates the 25.8 ms time point. Right: topography plot of the averaged potential at the electrodes for $t = 25.8$ ms

Fieldtrip¹⁰, FSL¹¹ and internal Matlab routines. We extracted surfaces from this voxel segmentation to distinguish between the different tissue compartments. To smooth the surfaces while maintaining the available information from the voxel segmentation, we applied an anti aliasing algorithm created for binary voxel images presented in [49]. The resulting smoothed surfaces are represented as level-set functions. The digitized electrodes were registered to the head surface using landmark-based rigid parametric registration. Especially in occipital and inferior regions, due to the lying position of the subject during MRI measurement, the gray matter compartment touches the inner skull surface. From Figure 4 we see a clear dipolar pattern in the topography plot. To estimate the location of the dipole, we performed a single dipole scan using a normal-constraint for dipole orientation on the source space, i.e., a set of source locations within the gray matter compartment [45]. The source space is created using a weighted sum of level-set functions for gray and white matter as $\alpha\Phi_{\text{wm}} + (1 - \alpha)\Phi_{\text{gm}}$ with $\alpha = 0.8$. The resulting level-set function for the source space was discretized using the marching cubes algorithm presented in [50], which resulted in 269 417 source locations. For each location, we computed the dipole orientation normal to the surface of the source space. Note that there was no manual interaction or modification of the surfaces obtained by this process. Figure 5 shows the skin, skull and gray matter surfaces and the electrode positions as well as the source space that was used in the example computation.

Using the level-set functions, we constructed a CutFEM head model and computed the EEG transfer matrix for all electrode positions using the presented duneuro toolbox. Using the transfer matrix, we computed the EEG forward solution for all dipole positions with the fixed orientation and unit strength using the Venant source model [38, 16]. The optimal strength s with respect to a given measurement m for a dipole with the leadfield l can be obtained by minimizing $\|ls - m\|_2$ over s . The resulting optimal strength for

¹⁰<http://fieldtriptoolbox.org>

¹¹<https://fsl.fmrib.ox.ac.uk/fsl>

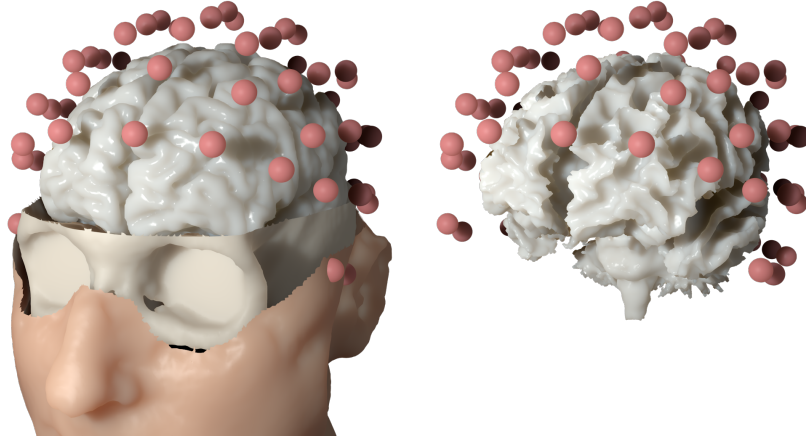


Figure 5: Left: skin, skull and gray matter surfaces of the six-compartment isotropic head model along with the electrode montage used in the practical example. Right: source space relative to the electrode positions.

reproducing the measured data is given as

$$s = \max \left(\frac{\langle l, m \rangle_2}{\|l\|_2^2}, 0 \right).$$

The maximum with 0 is used in order to restrict the solution along the respective positive normal direction because the P20/N20 component is assumed to be located in Brodmann area 3b of the somatosensory SI cortex pointing out of the cortex to produce a frontal positivity [51]. This strength is embedded into the goodness of fit measure (GOF) that is defined as

$$\text{GOF} = 1 - \frac{\|ls - m\|_2^2}{\|m\|_2^2}$$

and measures the ability of the numerical solution to reproduce the measured data. In the case of a single dipole scan this includes how well the data can be represented as a single dipole. Former results have shown that the single dipole source model is appropriate for the reconstruction of the early somatosensory response [52, 53, 51]. If the data can be exactly reproduced, the GOF has a value of 1. Figure 6 shows the source with the maximal GOF measure on three slices of the subjects MRI data. The GOF for this source is 0.974. The source was reconstructed in the primary somatosensory cortex in the wall of the post-central gyrus and has a mainly tangential orientation, which reproduces findings of [52, 53, 51]. Figure 7 shows the source embedded in the source

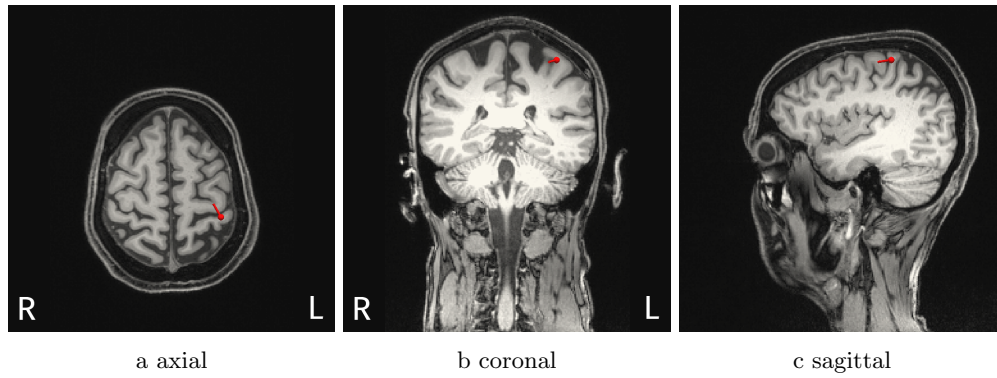


Figure 6: Reconstructed source (red) of the P20 component on an axial, a coronal and a sagittal slice of the MRI following electric stimulation of the medianus nerve at the right wrist. Note the left-right orientation of the axial and coronal slices following radiological convention.

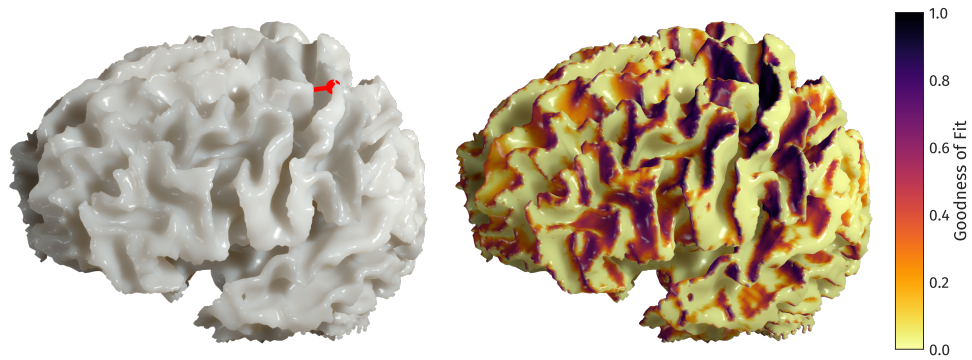


Figure 7: Left: Reconstructed source (red) of the P20 component and its location within the source space. Right: Distribution of the GOF measure on the source space. A darker color indicates a higher GOF.

space along the distribution of the GOF measure. We see that the GOF measure is higher for source locations on the gyral walls with a tangentially oriented normal vector and that the higher values are located close to the central sulcus. Overall, the GOF measure shows a smooth distribution in these areas while being sensitive to orientation changes.

7 Summary and Outlook

In this paper we presented the duneuro software, a toolbox for solving forward problems in neuroscience. We provided a general description of the toolbox as well as detailed information on the main concepts. Short examples showed the extendibility of the different subcomponents. We presented a method to efficiently localize positions within a given mesh and described bindings of the library for scripting languages. Finally the practical usability of the library was demonstrated by a source analysis of experimental data of a somatosensory stimulation. The duneuro toolbox offers a flexible and efficient way to solve the EEG/MEG forward problem using modern mathematical methods. There are several open goals regarding the software implementation. Foremost, a direct comparison with existing tools for computing forward solutions for EEG and MEG, such as the SimBio toolbox, is currently performed. Similar to the latter toolbox, a closer integration into existing source analysis frameworks, such as FieldTrip, BrainStorm or mne-python should be considered. This would also then allow to evaluate the advantages and disadvantages of the new FEM methods that are now available through the duneuro code in practical applications. This integration would offer the use of duneuro for different inverse approaches. Several other forward problems, e.g., electric or magnetic brain stimulation, are already partly implemented, but their support should be improved and evaluated. Of special interest would then be a connection to optimization procedures for transcranial direct current stimulation [54, 55]. In order to improve the stability of the codebase and ensure the reliability of the results even under future modifications, a testing framework using continuous integration should be implemented.

Acknowledgements

This work was supported by EU project ChildBrain (Marie Curie Innovative Training Networks, grant agreement 641652), by the Cluster of Excellence 1003 of the Deutsche Forschungsgemeinschaft (DFG EXC 1003 Cells in Motion), by the Deutsche Forschungsgemeinschaft (DFG), project WO1425/7-1 and by the Priority Program 1665 of the DFG (WO1425/5-2). SP and TM were supported by the Academy of Finland key project (305055) and TM also by the tenure track funding by Tampere University of Technology.

References

- [1] Brette R, Destexhe A. Handbook of neural activity measurement. Cambridge University Press; 2012.
- [2] Hallez H, Vanrumste B, Grech R, Muscat J, De Clercq W, Vergult A, et al. Review on solving the forward problem in EEG source analysis. *Journal of neuroengineering and rehabilitation*. 2007;4(1):46.
- [3] Oostenveld R, Fries P, Maris E, Schoffelen JM. FieldTrip: open source software for advanced analysis of MEG, EEG, and invasive electrophysiological data. *Computational intelligence and neuroscience*. 2011;2011:1.
- [4] Tadel F, Baillet S, Mosher JC, Pantazis D, Leahy RM. Brainstorm: a user-friendly application for MEG/EEG analysis. *Computational intelligence and neuroscience*. 2011;2011:8.
- [5] He Q, Rezaei A, Pursiainen S. Zeffiro user interface for electromagnetic brain imaging: a GPU accelerated FEM tool for forward and inverse computations in Matlab. *arXiv preprint arXiv:181107717*. 2018;.
- [6] Gramfort A, Luessi M, Larson E, Engemann DA, Strohmeier D, Brodbeck C, et al. MEG and EEG data analysis with MNE-Python. *Frontiers in neuroscience*. 2013;7:267.
- [7] Gramfort A, Luessi M, Larson E, Engemann DA, Strohmeier D, Brodbeck C, et al. MNE software for processing MEG and EEG data. *NeuroImage*. 2014;86:446 – 460. Available from: <http://www.sciencedirect.com/science/article/pii/S1053811913010501>.
- [8] Vorwerk J, Oostenveld R, Piastra MC, Magyari L, Wolters CH. The FieldTrip-SimBio pipeline for EEG forward solutions. *BioMedical Engineering OnLine*. 2018;17(1):37.
- [9] Bastian P, Blatt M, Dedner A, Engwer C, Klöfkorn R, Ohlberger M, et al. A generic grid interface for parallel and adaptive scientific computing. Part I: abstract framework. *Computing*. 2008;82(2-3):103–119.
- [10] Bastian P, Blatt M, Dedner A, Engwer C, Klöfkorn R, Kornhuber R, et al. A generic grid interface for parallel and adaptive scientific computing. Part II: implementation and tests in DUNE. *Computing*. 2008;82(2-3):121–138.
- [11] Bastian P, Birken K, Johannsen K, Lang S, Neuß N, Rentz-Reichert H, et al. UG—a flexible software toolbox for solving partial differential equations. *Computing and Visualization in Science*. 1997;1(1):27–40.

- [12] Wolters CH, Anwander A, Berti G, Hartmann U. Geometry-Adapted Hexahedral Meshes Improve Accuracy of Finite-Element-Method-Based EEG Source Analysis. *IEEE Transactions on Biomedical Engineering*. 2007 Aug;54(8):1446–1453.
- [13] Gräser C, Sander O. The dune-subgrid module and some applications. *Computing*. 2009;86(4):269.
- [14] Bastian P, Heimann F, Marnach S. Generic implementation of finite element methods in the distributed and unified numerics environment (DUNE). *Kybernetika*. 2010;46(2):294–315.
- [15] Engwer C, Heimann F. Dune-udg: A cut-cell framework for unfitted discontinuous galerkin methods. In: *Advances in DUNE*. Springer; 2012. p. 89–100.
- [16] Nüßing A. Fitted and Unfitted Finite Element Methods for Solving the EEG Forward Problem [Ph.D. thesis]. Westfälische Wilhelms-Universität Münster; 2018.
- [17] Blatt M, Bastian P. The iterative solver template library. In: *International Workshop on Applied Parallel Computing*. Springer; 2006. p. 666–675.
- [18] Brenner S, Scott R. The mathematical theory of finite element methods. vol. 15. Springer Science & Business Media; 2007.
- [19] Gençer NG, Acar CE. Sensitivity of EEG and MEG measurements to tissue conductivity. *Physics in Medicine & Biology*. 2004;49(5):701.
- [20] Lew S, Wolters C, Dierkes T, Röer C, MacLeod R. Accuracy and run-time comparison for different potential approaches and iterative solvers in finite element method based EEG source analysis. *Applied Numerical Mathematics*. 2009;59(8):1970–1988.
- [21] Medani T, Lautru D, Schwartz D, Ren Z, Sou G. FEM method for the EEG forward problem and improvement based on modification of the saint venant’s method. *Progress In Electromagnetics Research*. 2015;153:11–22.
- [22] Pursiainen S, Sorrentino A, Campi C, Piana M. Forward simulation and inverse dipole localization with the lowest order Raviart—Thomas elements for electroencephalography. *Inverse Problems*. 2011;27(4):045003.
- [23] Schimpf PH, Ramon C, Haueisen J. Dipole models for the EEG and MEG. *IEEE Transactions on Biomedical Engineering*. 2002;49(5):409–418.
- [24] Weinstein D, Zhukov L, Johnson C. Lead-field bases for electroencephalography source imaging. *Annals of biomedical engineering*. 2000;28(9):1059–1065.
- [25] Beltrachini L. A finite element solution of the forward problem in EEG for multipolar sources. *IEEE Transactions on Neural Systems and Rehabilitation Engineering*. 2018;.

- [26] Beltrachini L. Sensitivity of the projected subtraction approach to mesh degeneracies and its impact on the forward problem in EEG. *IEEE Transactions on Biomedical Engineering*. 2019;66(1):273–282.
- [27] Acar ZA, Acar CE, Makeig S. Simultaneous head tissue conductivity and EEG source location estimation. *NeuroImage*. 2016;124:168–180.
- [28] Marin G, Guerin C, Baillet S, Garnero L, Meunier G. Influence of skull anisotropy for the forward and inverse problem in EEG: simulation studies using FEM on realistic head models. *Human brain mapping*. 1998;6(4):250–269.
- [29] Van Uitert R, Johnson C, Zhukov L. Influence of head tissue conductivity in forward and inverse magnetoencephalographic simulations using realistic head models. *IEEE Transactions on Biomedical Engineering*. 2004;51(12):2129–2137.
- [30] Vallaghé S, Papadopoulou T. A trilinear immersed finite element method for solving the electroencephalography forward problem. *SIAM Journal on Scientific Computing*. 2010;32(4):2379–2394.
- [31] Engwer C, Vorwerk J, Ludewig J, Wolters CH. A Discontinuous Galerkin Method to Solve the EEG Forward Problem Using the Subtraction Approach. *SIAM Journal on Scientific Computing*. 2017;39(1):B138–B164.
- [32] Vorwerk J, Engwer C, Pursiainen S, Wolters CH. A mixed finite element method to solve the EEG forward problem. *IEEE transactions on medical imaging*. 2017;36(4):930–941.
- [33] Burman E, Claus S, Hansbo P, Larson MG, Massing A. CutFEM: Discretizing Geometry and Partial Differential Equations. *International Journal for Numerical Methods in Engineering*. 2015;104(7):472–501.
- [34] Bastian P, Engwer C. An unfitted finite element method using discontinuous Galerkin. *Int J Numer Methods Eng*. 2009;79(12):1557–1576.
- [35] Gürkan C, Massing A. A stabilized cut discontinuous Galerkin framework: I. Elliptic boundary value and interface problems. *arXiv preprint arXiv:180306635*. 2018;.
- [36] Nüßing A, Wolters CH, Brinck H, Engwer C. The Unfitted Discontinuous Galerkin Method for Solving the EEG Forward Problem. *IEEE Transactions on Biomedical Engineering*. 2016 Dec;63(12):2564–2575.
- [37] Yan Y, Nunez P, Hart R. Finite-element model of the human head: scalp potentials due to dipole sources. *Medical and Biological Engineering and Computing*. 1991;29(5):475–481.

- [38] Vorwerk J, Cho JH, Rampp S, Hamer H, Knösche TR, Wolters CH. A guideline for head volume conductor modeling in EEG and MEG. *NeuroImage*. 2014;100:590–607.
- [39] Drechsler F, Wolters CH, Dierkes T, Si H, Grasedyck L. A Full Subtraction Approach for Finite Element Method Based Source Analysis Using Constrained Delaunay Tetrahedralisation. *NeuroImage*. 2009 Jul;46(4):1055–1065.
- [40] Bauer M, Pursiainen S, Vorwerk J, Köstler H, Wolters CH. Comparison study for Whitney (Raviart–Thomas)-type source models in finite-element-method-based EEG forward modeling. *IEEE Transactions on Biomedical Engineering*. 2015;62(11):2648–2656.
- [41] Pursiainen S, Vorwerk J, Wolters CH. Electroencephalography (EEG) forward modeling via H (div) finite element sources with focal interpolation. *Physics in Medicine & Biology*. 2016;61(24):8502.
- [42] Miinalainen T, Rezaei A, Us D, Nüßing A, Engwer C, Wolters CH, et al. A realistic, accurate and fast source modeling approach for the EEG forward problem. *NeuroImage*. 2019;184:56–67.
- [43] Vorwerk J. New finite element methods to solve the EEG/MEG forward problem [Ph.D. thesis]. Westfälische Wilhelms-Universität Münster; 2016.
- [44] Piastra MC, Nüßing A, Vorwerk J, Bornfleth H, Oostenveld R, Engwer C, et al. The Discontinuous Galerkin Finite Element Method for Solving the MEG and the Combined MEG/EEG Forward Problem. *Frontiers in Neuroscience*. 2018;12:30.
- [45] Hämmäläinen M, Hari R, Ilmoniemi RJ, Knuutila J, Lounasmaa OV. Magnetoencephalography—theory, instrumentation, and applications to noninvasive studies of the working human brain. *Reviews of modern Physics*. 1993;65(2):413.
- [46] Brown PJ, Faigle CT. A robust efficient algorithm for point location in triangulations. University of Cambridge, Computer Laboratory; 1997.
- [47] Bentley JL. Multidimensional binary search trees used for associative searching. *Communications of the ACM*. 1975;18(9):509–517.
- [48] Rice JK, Rorden C, Little JS, Parra LC. Subject position affects EEG magnitudes. *NeuroImage*. 2013;64:476–484.
- [49] Whitaker RT. Reducing aliasing artifacts in iso-surfaces of binary volumes. In: *Proceedings of the 2000 IEEE symposium on Volume visualization*. ACM; 2000. p. 23–32.
- [50] Engwer C, Nüßing A. Geometric Reconstruction of Implicitly Defined Surfaces and Domains with Topological Guarantees. *ACM Transactions on Mathematical Software (TOMS)*. 2017;44(2):14.

- [51] Aydin Ü, Vorwerk J, Küpper P, Heers M, Kugel H, Galka A, et al. Combining EEG and MEG for the reconstruction of epileptic activity using a calibrated realistic volume conductor model. *PLoS One*. 2014;9(3):e93154.
- [52] Allison T, McCarthy G, Wood CC, Jones SJ. Potentials evoked in human and monkey cerebral cortex by stimulation of the median nerve: a review of scalp and intracranial recordings. *Brain*. 1991;114(6):2465–2503.
- [53] Nakamura A, Yamada T, Goto A, Kato T, Ito K, Abe Y, et al. Somatosensory homunculus as drawn by MEG. *Neuroimage*. 1998;7(4):377–386.
- [54] Dmochowski JP, Datta A, Bikson M, Su Y, Parra LC. Optimized multi-electrode stimulation increases focality and intensity at target. *Journal of neural engineering*. 2011;8(4):046011.
- [55] Wagner S, Burger M, Wolters CH. An optimization approach for well-targeted transcranial direct current stimulation. *SIAM Journal on Applied Mathematics*. 2016;76(6):2154–2174.